9th International Conference on Nuclear Engineering
ICONE-9
April 8-12, 2001

STATUS OF EMERGENCY SPRAY MODELLING IN THE INTEGRAL CODE ASTEC

William Plumecocq
Institut de Protection et de Sûreté Nucléaire
Département de Recherches en Sécurité
CE Cadarache 13108 St Paul lez Durance Cedex France
e-mail: plumecoc@sand.cad.cea.fr

Roberto Passalacqua
ENEA Dipartimento Energia,
ENEA CR Casaccia, via Anguillarese 301, 00060 Rome, Italy
e-mail: roberto.passalacqua@casaccia.enea.it

KEYWORDS: ASTEC Code, Spray System, Severe Accidents, Accident Management

ABSTRACT

Containment spray systems are emergency systems that would be used in very low probability events which may lead to severe accidents in Light Water Reactors. In most cases, the primary function of the spray would be to remove heat and condense steam in order to reduce pressure and temperature in the containment building. Spray would also wash out fission products (aerosols and gaseous species) from the containment atmosphere.

The efficiency of the spray system in the containment depressurisation as well as in the removal of aerosols, during a severe accident, depends on the evolution of the spray droplet size distribution with the height in the containment, due to kinetic and thermal relaxation, gravitational agglomeration and mass transfer with the gas. A model has been developed taking into account all of these phenomena.

This model has been implemented in the ASTEC code with a validation of the droplets relaxation against the CARAIDAS experiment (IPSN). Applications of this modelling to a PWR 900, during a severe accident, with special emphasis on the effect of spray on containment hydrogen distribution have been performed in multi-compartment configuration with the ASTEC V0.3 code.

INTRODUCTION

During a severe accident, the efficiency of the spray system in the containment depressurisation as well as in the aerosols removal depends on the evolution of the droplet size distribution with the height in the containment, due to kinetic and thermal relaxation, gravitational agglomeration and mass transfer with the gas. A model (Plumecocq 1997) has been developed taking into account all of these phenomena. This model has been partly validated against the CARAIDAS experiment (IPSN). This facility is aimed at measuring collection efficiencies for droplets having a well-defined size and velocity at injection in an atmosphere with steady, homogeneous conditions. Preliminary tests were devoted to droplet relaxation kinetics in superheated conditions.

This model (except gravitational agglomeration) has been implemented in the ASTEC code (Accident Source Term Evaluation Code) which is under development by Institut de Protection et de Sûreté Nucleaire (IPSN), France, and Gesellschaft für Anlagen-und Reaktorsicherheit (GRS), Germany. The aim of the development is to create a fast running integral code package for the simulation of the whole course of severe accidents in light-water reactors.

Spray modelling, as implemented in ASTEC V0.3 code, has been evaluated in multi-compartment configurations of a PWR 900 MWe during a prototypical high pressure -melt ejection accident.

SPRAY MODELLING

The evolution of a droplet during its fall (mass, velocity and temperature) is obtained by solving a set of equations for mass, momentum and energy balance :

$$\frac{dm_w}{dz} = \pi d_w \, Sh_g \, \overline{D}_s \, \overline{c}_g \, M_w \, B_M / v_w$$

$$\frac{d}{dz}(m_w v_w) = m_w \, g / v_w - \frac{\pi d_w^2}{8} C_D \, \rho_g \, v_w$$

$$\frac{d}{dz}(m_w H_w) = (\pi d_w \, \lambda_g \, Nu_g \, (T_g - T_w))/v_w + \frac{dm_w}{dz} H_s$$

z : height

B_M Spalding number for mass transfer :

$$B_M = \frac{X_{s\infty} - X_{sw}}{1 - X_{sw}}$$

$\overline{c}_g$ average steam-air mixture molar concentration

$\overline{D}_s$ average steam-air diffusion coefficient

d_w droplet diameter

H_s specific enthalpy of steam

H_w specific enthalpy of water

m_w droplet mass

M_w water molar mass

T_w droplet temperature

v_w droplet velocity

λ_g steam-air mixture thermal conductivity

ρ_g gas density

g acceleration due to gravity

$X_{s\infty}$ molar fraction of steam in the bulk fluid

X_{sw} molar fraction of steam at droplet surface

Knowing the atmosphere conditions and the injection conditions of droplets (velocity, diameter, temperature), the dynamics of droplets is defined by the expression of the three nondimension numbers (Sh_g, Nu_g, C_D). The Nusselt number Nu_g and Sherwood number Sh_g were deduced from steady evaporation in dry air of droplets having diameters in the range 600 to 1100 microns (Ranz and Marshall, 1952) :

$$Sh_g = 2 + 0.6\,Re_w^{1/2}\,Sc_g^{\ 1/3}$$

$$Nu_g = 2 + 0.6\,Re_w^{1/2}\,Pr_g^{\ 1/3}$$

Pr_g steam-air mixture Prandtl number

Re_w droplet Reynolds number

Sc_g steam-air mixture Schmidt number

The drag coefficient C_D is taken from the Oseen formulation (Hinds, 1982) for hard spheres :

for $Re_w < 3$ $\quad C_D = 24 / Re_w$ (Stokes flow)

for $3 < Re_w < 905$ $\quad C_D = \frac{24}{Re_w}\left(1 + \frac{Re_w^{2/3}}{6}\right)$

for $Re_w > 905$ $\quad C_D = 0.44$ (potential flow)

This set of equations is solved on a fixed meshing by using an implicit numerical scheme and the Euler method.

Mass and energy balance

The rates of transfer between atmosphere and droplets are strongly dependent on the droplets size. To characterise the droplets size distribution, one introduces the concept of distribution function f(r) whose properties are comparable with those of a density of probability. This function is such as the number of droplets per unit of volume whose radius lies between r and r + dr is:

$$dn = f(r)\,dr$$

The droplets size distribution produced by the Sprayco spray nozzle (Model 1713-A), typically used in PWRs, is well represented by a log-normal distribution function :

$$f(r) = \frac{n_0}{\sqrt{2\pi}\,\ln\sigma\, r}\exp\left[-\frac{\left(\ln\frac{r}{r_g}\right)^2}{2\,(\ln\sigma)^2}\right] \quad (m^{-4})$$

r_g geometric radius

σ standard deviation

n_0 number concentration of droplets

The time evolution of the thermal-hydraulic conditions in a containment compartment (pressure, temperature, relative humidity) due to the spray is obtained from a mass and energy balance. This balance corresponds to the mass and enthalpy removed by spray droplets during their fall. This one is determined from the droplet behaviour results and the evolution of the droplets distribution function between the top and the bottom of the compartment as follows :

$$\frac{d\rho_s}{dt} = -\frac{1}{h}\left(\int f(x,h)\,m_w(x,h)\,v_w(x,h)\,dx - \int f(x,0)\,m_w(x,0)\,v_w(x,0)\,dx\right)$$

$$\frac{dU}{dt} = -\frac{1}{h}\left(\int f(x,h)\,m_w(x,h)\;H_w(x,h)\,v_w(x,h)\,dx - \int f(x,0)\,m_w(x,0)\;H_w(x,0)\,v_w(x,0)\,dx\right)$$

U internal energy of gas per unit of volume

ρ_s density of steam

x droplet size class

h height of the compartment

Aerosols collection

The so-called mechanical collection is due to inertial impaction for large aerosols and to diffusion for small aerosols. The impaction mechanism is linked to the trajectories of particles which do not follow streamlines while diffusion is linked to the thickness of the boundary layer around the droplet in which a particle concentration gradient is established. Particles of intermediate size (between 0.1 and 1 micron diameter) follow the streamlines but can be collected due to their finite size (interception).

Inertial impaction efficiency is expressed in terms of the Stokes number. The Langmuir and Blodgett correlation (Langmir and Blodgett, 1946) has been retained on the basis of numerical simulations for the potential and viscous flow regimes. Beard and Grover (beard and Grover, 1974) proposed an interpolation formulation for the intermediate regime based on numerical simulations. This correlation provides satisfactory agreement with experimental data (Ranz and Wong, 1952), (Walton and Woolcock, 1960).

Fuchs (Fuchs, 1964) calculated analytically a correction to the impaction efficiency taking into account the interception effect :

$$\varepsilon = \varepsilon_{imp} + 3\frac{d_p}{d_w} \quad \text{for potential flow}$$

$$\varepsilon = \varepsilon_{imp} + \frac{3}{2}\left(\frac{d_p}{d_w}\right)^2 \quad \text{for viscous flow}$$

For the collection efficiency due to diffusion, no experimental data are available in the literature. It is expressed in terms of the droplet Reynolds number and particle Peclet number. The only available formulation is based on the analogy between particle and molecular diffusion, (Ranz and Marshall, 1952) , in which the molecular steam-air diffusion coefficient is replaced by the particle diffusion coefficient. We retained the Postma formulation (Postma, 1975) in which the boundary layer thickness is corrected in order to take into account the finite particle size.

Phoretic effects are expressed in term of deposition velocity. It is converted into collection efficiency assuming a spherical flow around the droplet (exact solution of the phoretic motion in the actual flow would be obtained by numerical simulations). The deposition velocity due to thermophoresis is related to the Nusselt number and atmosphere-droplet temperature difference by using the Brock (Brock,1962) or Talbot formulation (Hidy et al, 1970). The drift velocity due to steam condensation or evaporation is related to the condensation or evaporation mass flow rate (Schmitt and Waldmann, 1966). The coupling between diffusive and phoretic effects is described by correcting the diffusive deposition velocity v_d in the following way (Plumecocq, 1997) :

$$v = v_d \, B(\chi)$$

where χ is the ratio of the phoretic velocity to the diffusive velocity and

$$B(\chi) = \frac{\chi}{1 - \exp(-\chi)}$$

This formulation has the correct limits and allows to have the deposition velocity going continuously to zero in case of evaporation.

VALIDATION

An experimental device named CARAIDAS (Vendel et al., 1998) was designed and built in order to determine the collection efficiency of aerosols and iodine absorption by droplets with representative conditions of post-accident atmosphere. CARAIDAS allows to measure experimental droplets diameter evolution and collected aerosols mass by falling droplets as a function of different experimental conditions. Droplets are injected with a well-defined size and velocity in an atmosphere with steady and homogeneous conditions. Preliminary tests were devoted to droplet relaxation kinetics in superheated conditions.

Experimental vessel

Experimental vessel is a 5 meters high cylinder with an inner diameter of 0.6 meter (see figure 1). The vessel is heated up by circulating a thermo-fluid through the double-wall casing. Homogeneous thermodynamic conditions are obtained by using an air-steam circulation. Steam saturation rate range is from a few percents till 95 % to avoid condensation on the inner surfaces. When nominal working conditions (pressure, temperature, saturation ratio) are reached, air-system circulation is stopped and the vessel is isolated.

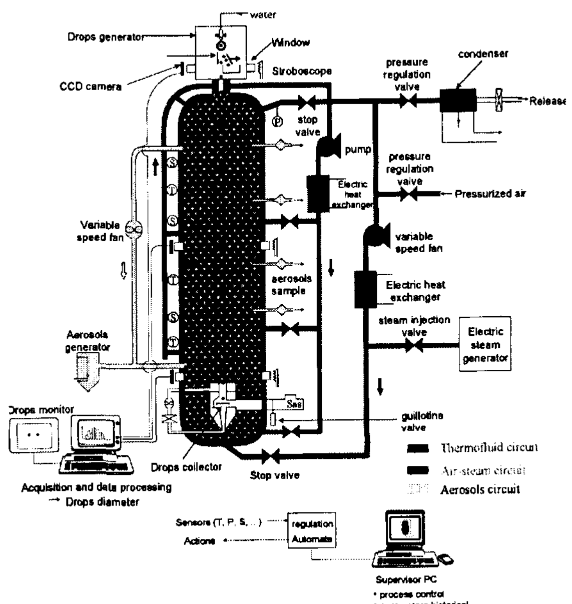

Figure 1: Experimental device CARAIDAS

Droplets generator is located at the top of the experimental vessel. In order to produce mono-sized droplets, the generator is based on a break-up process of a jet to droplets by applying a periodic disturbance. This device can produce mono-sized water droplets with a diameter ranging from 200 to 700 μm.

After injection into the vessel, the droplets diameter is modified by steam condensation or evaporation as function of thermodynamic conditions. Optical measurements of the droplets diameter are performed at three elevations : one at the top of the vessel where the droplets are emitted (z = 0 m), a second one at mid-height (z = 2,51 m) and the last one at the bottom of the device (z = 4,39 m). At the end of the fall, droplets are collected to measure the aerosols mass removed.
Aerosols generation is based on mechanical spraying by a rotative disk. Aerosols diameter range is between 0.5 and 5 μm with a geometric standard deviation lower than 2.

Results

Acquisition of experimental results on the device CARAIDAS allows to qualify the modelling of the droplets behaviour. During these tests, a large range of experimental conditions was achieved in the experimental vessel (pressure from 1 bar to 7 bar, temperature from 20 °C to 160 °C and relative humidity from few percent till 95%). For each test, measurements of mean droplet diameter and standard deviation of droplets are performed at the three measurements levels. Results of the droplets relaxation are shown on figures 2 through 5.

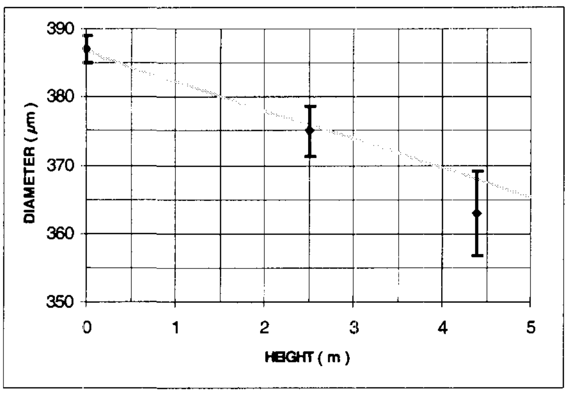

Figure 2 : droplet size evolution
for a gas at 1 bar, 47 °C and RH 12 %.

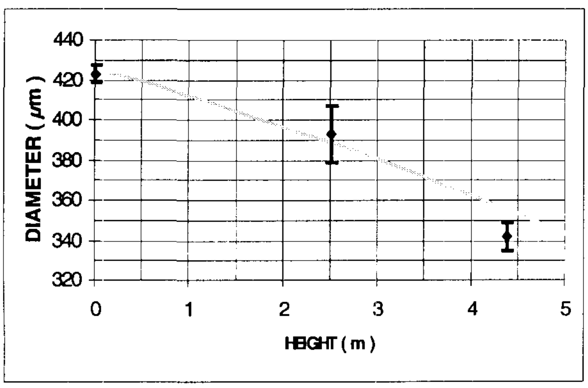

Figure 3 : droplet size evolution
for a gas at 1 bar, 146.6 °C and RH <1 %

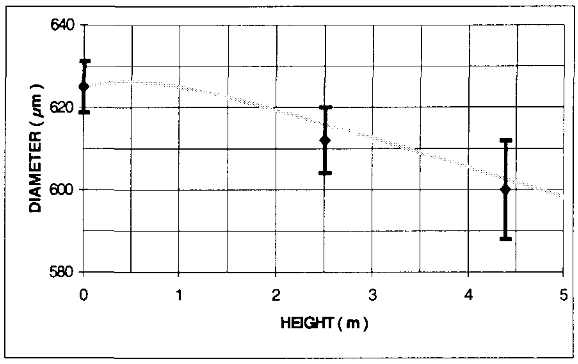

Figure 4 : droplet size evolution
for a gas at 2.4 bar, 99 °C and RH 6.3 %

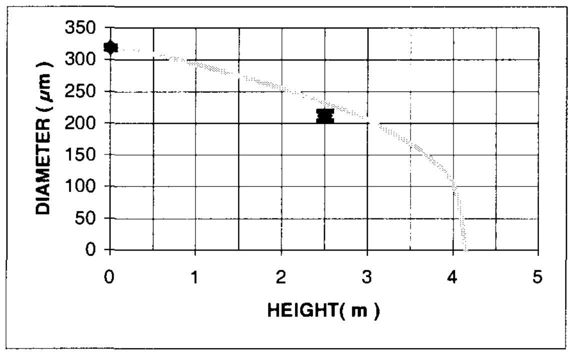

Figure 5 : droplet size evolution
for a gas at 3.2 bar, 135 °C and RH 2.3 %

With the formulation of the mass, momentum and heat transfer described above, we obtain a fairly good prediction of the droplet dynamic tests performed in CARAIDAS.
Figure 4 shows that steam condensation on droplet occurs at the beginning of the fall : heat and mass flow rates induce the growth and the heating of the droplet. When the droplet temperature reaches the dew temperature, steam condensation stops. As this temperature is lower than the gas temperature (RH <100 %), evaporation occurs : there is an equilibrium between the heat flow transferred to the droplet and the heat lost by evaporation. Thus, the droplet temperature remains steady while its diameter decreases.
In the figure 5, droplets disappear before they reach the vessel bottom. This complete droplet evaporation is well predicted by the model.

REACTOR APPLICATIONS

The spray model has been implemented in the ASTEC code. An application on a French REP 900 nuclear plant has been performed with 16 containment nodes (see figure 6). The dome, rather than one single physical compartment, is modelled by 6 gaseous sub-volumes belonging to the same physical compartment.

The accident sequence here studied is a high pressure-melt ejection sequence.

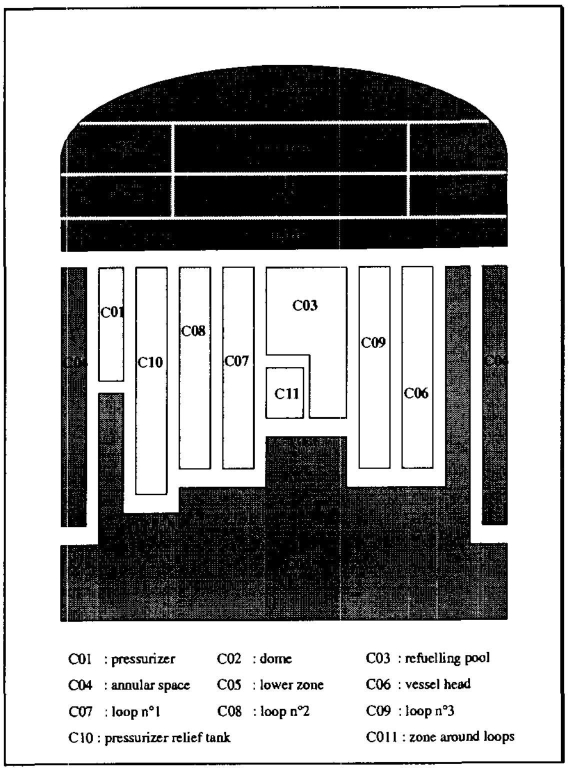

Figure 6 : containment nodalisation

Sequence description

This sequence is called H2 (in the French accident sequence nomenclature), better known as a TMLB sequence. The initiator event is loss of steam generator feed water and a simultaneous unavailability of the emergency core cooling system (ECCS) is assumed. Steam generators dry out, core heats up and PORVs open in order to avoid a too large pressurisation of primary system.

Vessel pressure ranges (by PORV regulation) between 160 and 165 bar. Accumulators do not intervene because primary system pressure remains high. During the core degradation phase, steam blow-down (thus, containment pressure) depends essentially on PORV regulation. Hydrogen, structural materials and fission products, under gaseous and aerosol form, are released (through the PORVs) into the compartment C10.

Because of the high primary system pressure, dry-out starts at about 5700 seconds. Total core dry-out is reached in about 2000 seconds (for comparison, in a large break LOCA sequence core dry-out starts at 2500 seconds and lasts about 1000 seconds).

Direct Containment Heating (DCH) occurs at the bottom head vessel failure: vessel pressure, which drives corium entrainment into the containment dome is about the operating pressure.

Sprays are assumed to operate at the vessel failure since at this time the pressure peak is much larger than sprays pressure set point (2.4 bar). Two paths (user input) have been defined for the description of the spray in the containment. The first path, which covers 80% of the gas exchange area is limited to the central part of the dome. Collected water at the floor will be drained from the dome directly to the lower compartment through junctions. The second path (20% of the exchange area) goes through the peripheral part of the dome, and then through the annulus (C04) to the lower compartment (C05). Heat and mass transfer between gas and spray droplets occur all along the second path. Furthermore, no splashing on structures is assumed although the possibility is included in the code.

Containment thermal-hydraulic behaviour

Containment atmosphere is strongly modified by spray. At the start of the spray, pressure drops to 1.5 bar and temperature to 50 °C against 3 bar and 120 °C without spray (figures 7 through 12).

Figure 9 shows that, in case sprays are not activated, saturation ratio is around 15 %. In the lower part of the dome (C02F), saturation ratio is larger because of the larger temperature of the cell (figure 11). In addition, the sump, developed in the lower cell of the dome, increases steam partial pressure.

Figure 10 shows the larger saturation ratio predicted when spray are operating. When sprays intervene, at the vessel failure (which is at about 11600 seconds) water droplets are initially strongly evaporated because of the very superheated containment atmosphere: steam blow-down is heated up to above 1000 °C by corium entrainment and metal oxidation (DCH). Droplets evaporation increases very rapidly the saturation ratio up to 100 % almost everywhere in the containment (figure 10).

After this transient, steam condensation occurs on water droplets during the first part of their fall (globally steam fraction strongly decreases: compare figures 13 and 14). However, droplets still evaporate in the last part of their fall reducing containment temperature.

Because of the large gas release (especially non-condensable gases) from MCCI, saturation ratio is decreasing again (figure 10). Only when corium metal oxidation is over, sprays lead towards more saturated conditions.

The last abrupt change in the saturation ratio, at about 20000 seconds (figure 10) is due to the switch from the direct mode to the re-circulation mode. Water droplets are suddenly injected at higher temperature (56 °C in our case) because sump water is used for the re-circulation mode. Consequently, a partial droplets evaporation is observed at the start of the re-circulation phase (figure 12).

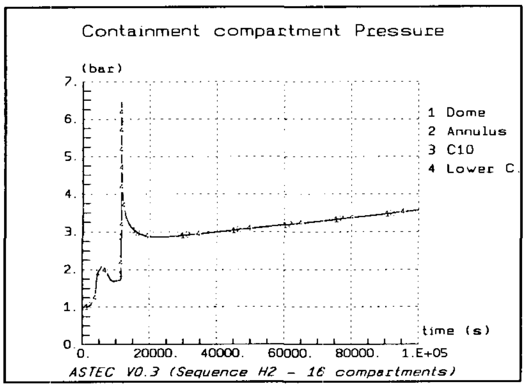

Figure 7: containment pressure – without spray

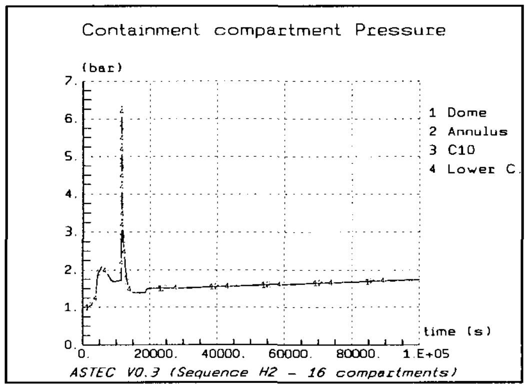

Figure 8: containment pressure – with spray

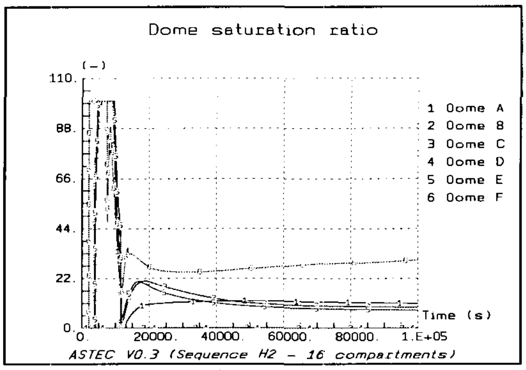

Figure 9: saturation ratios – without spray

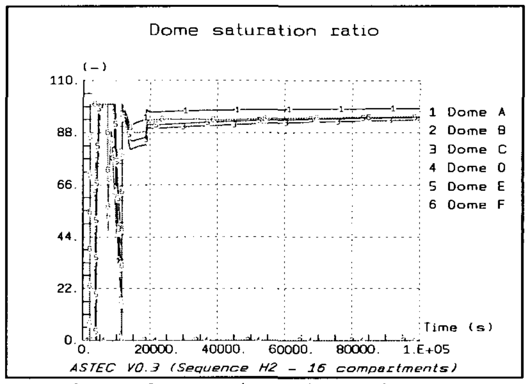

Figure 10: saturation ratios – with spray

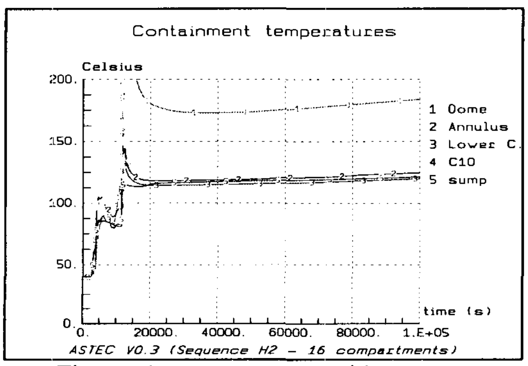

Figure 11: temperatures – without spray

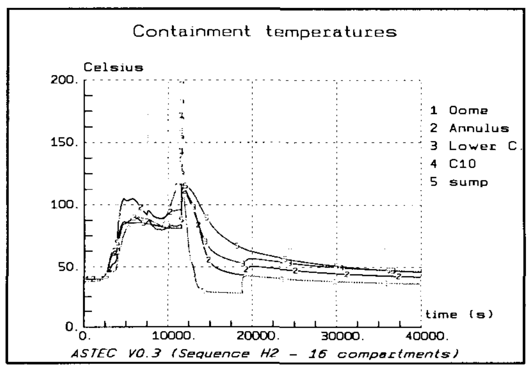

Figure 12: temperatures – with spray

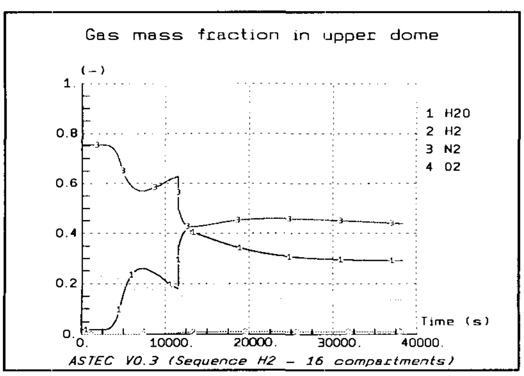

Figure 13: steam fraction – without spray

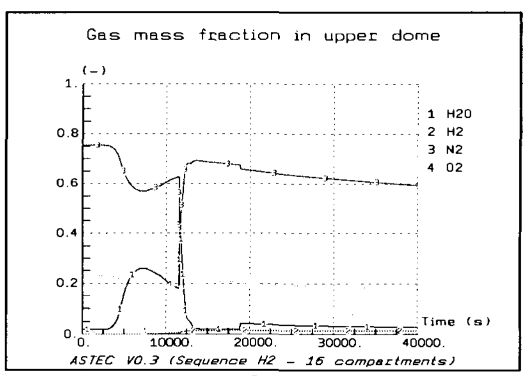

Figure 14: steam fraction – with spray

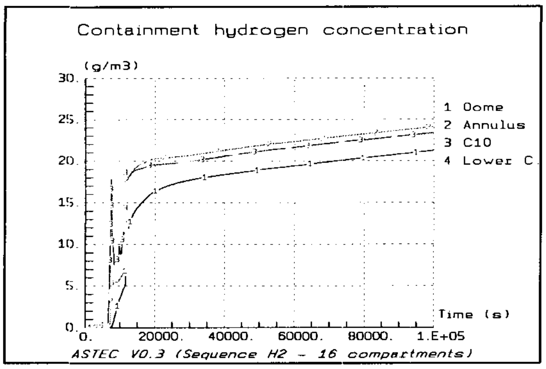

Figure 15: hydrogen concentration – without spray

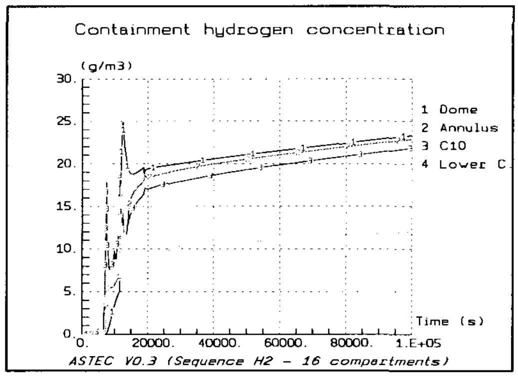

Figure 16: hydrogen concentration – with spray

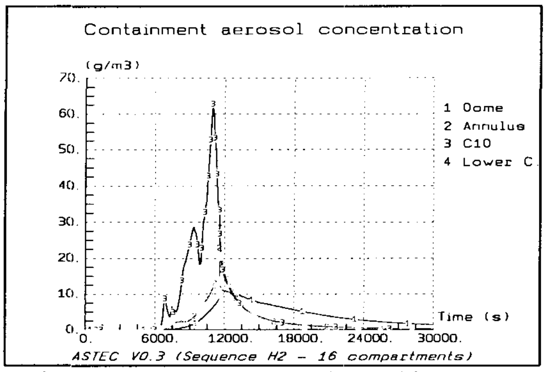

Figure 17: aerosol concentration– without spray

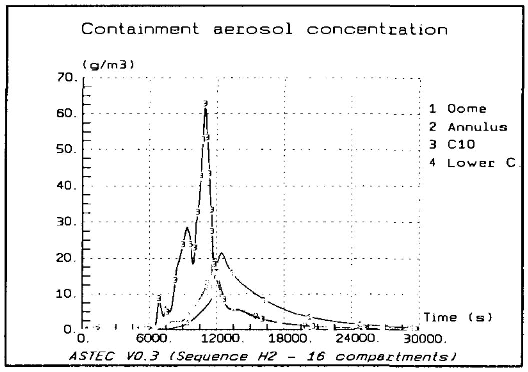

Figure 18: aerosol concentration– with spray

Spray influence on hydrogen risk

Figure 15 shows hydrogen concentrations attaining 20 g/m^3 at the vessel failure occurrence, without spray intervention. These concentrations are enough to cause H_2 combustion. In case of spray activation, higher hydrogen concentrations are observed in the dome (about 25 g/m^3). This is due to the hydrogen relocalisation at the start of the spray (compare figures 15 and 16). At this time, spray is very effective. After a short period during which spray droplets evaporate, the zone located just below spray nozzles is depleted in steam due to the steam condensation and consequently enriched in non-condensable gases to keep a constant total pressure (see figures 13 and 14).

Spray influence on aerosol removal

Figures 17 and 18 show the aerosol concentration in suspension in the containment (figure 17 refers to a calculation without spray). Concentration in the upper dome decreases much faster when sprays are operated (figure 18). However, as the sprays start, aerosol transport is promoted in the upper part of the dome and concentration almost doubles in this zone from 10 to 20 g/m^3. This is due again to steam condensation on water droplets that occurs essentially in the upper dome. Thus, a driving force for aerosol transport exist as long as important steam partial pressure differences are predicted. At the same time, aerosol concentration decreases in the other compartments due to gas transfer to the upper dome (figure 18).

CONCLUSION

A modelling of the containment spray system has been developed, taking into account the evolution of the droplet size distribution with the height in the containment, due to kinetic and thermal relaxation, and mass transfer with the gas. This model has been implemented in the ASTEC code with a validation of the droplets relaxation against the CARAIDAS experiment. Experimental results showed a good agreement with theory. Nevertheless, a confirmation will be necessary on the TOSCAN experiment (IPSN) more representative of the containment spray system. The model of aerosol removal by spray droplets is going to be validated on CARAIDAS results.

Applications of this modelling to a PWR 900 MWe during a severe accident, with the ASTEC V0.3 code using a multi-compartment configuration have been performed.

The spray model has shown a good robustness and flexibility with a good degree of physical modelling. Spray behaviour has been evaluated when simultaneous and complex accident sequence occurrences are modelled as DCH and MCCI.

The analysis of spray behaviour during a severe accident has given some insights on the evaluation of the hydrogen risk and some insights for the management of the accident and for the installation of safety related devices as for example hydrogen recombiners.

ACKNOWLEDGMENTS

The authors are very grateful to Jacques Vendel (IPSN) for the availability of the CARAIDAS experimental results and Victor Layly, (IPSN) for fruitful discussions and its contribution on the modelling of aerosol collection by spray.

REFERENCES

1. W. Plumecocq "Etude de l'interaction d'un système d'aspersion liquide avec l'atmosphère environnante", thèse Université de Provence , Marseille (1997)
2. W.E. Ranz, W.R. Marshall "Evaporation from drops", Chemical Engineering Progress vol 48 n°3 141-146, n°4 173-180 (1952)
3. W.C. Hinds "Aerosol Technology" Wiley Interscience Publication (1982)
4. I. Langmuir, K. Blodgett, U.S. Air Force technical report 5418 (1946)
5. W. Ranz, J. Wong, "Impaction of Dust and Smoke Particles on Surface and Body Collectors", Industrial and Engineering Chemistry, Vol.44, (1952)
6. W. H. Walton, A. Woolkock "The superposition of airborne dust by water spray", Int. J. Air Pollut., 3 : 129-152 (1960)
7. N. A. Fuchs "The Mechanics of Aerosols", Dover Publications New York 1964
8. A. K. Postma "Models for Predicting the Removal of Airborne Contaminants by Reactor Containment Spray", BNWL-B-417, (1975)
9. J. R. Brock "On the Theory of Thermal Forces Acting on aerosol Particles", J. of Coll. Sci., 17, 768, (1962).
10. G. M. Hidy, J. R. Brock, "The dynamics of aerocolloidal systems", Vol.1, Pergamon Press, New York (1970)
11. L. Waldmann, K. H. Schmitt "Thermophoresis and Diffusiophoresis of Aerosols" Chap.6 of Aerosol Science, Edited by C.N. Davies, Academic Press, New York, (1966)
12. J. Vendel et al. "Aerosols collection by spray water drops : experimental results and model" Cooperative Severe Accident Research Program meeting. May 1998, Bethesda, Maryland USA
13 K. Beard, S. Grover "Numerical collision efficiencies for small raindrops colliding with micron size particles" Journal of the atmospheric science (1974)